



Lawrence Berkeley National Laboratory

Assessment of occupant-behavior-based indoor air quality and its impacts on human exposure risk: A case study based on the wildfires in Northern California

Na Luo^{1,2,3}, Wenguo Weng^{1,2*}, Xiaoyu Xu^{1,2}, Tianzhen Hong³, Ming Fu⁴, Kaiyu Sun³

¹ Institute of Public Safety Research, Department of Engineering Physics, Tsinghua University, Beijing, 100084, P.R. China

² Beijing Key Laboratory of City Integrated Emergency Response Science, Tsinghua University, Beijing, 100084, China.

³ Building Technology and Urban Systems Division, Lawrence Berkeley National Laboratory, USA

⁴ Hefei Institute for Public Safety Research, Tsinghua University, Hefei, Anhui Province, 320601, China.

Energy Technologies Area

October 2019

For citation, please use:

Luo, N., Weng, W., Xu, X., Hong, T., Fu, M., Sun, K. 2019 Assessment of occupant-behavior-based indoor quality and its impacts on human exposure risk: A case study based on the wildfires in Northern California. *Science of the Total Environment*. <https://doi.org/10.1016/j.scitotenv.2019.05.467>

Disclaimer:

This document was prepared as an account of work sponsored by the United States Government. While this document is believed to contain correct information, neither the United States Government nor any agency thereof, nor the Regents of the University of California, nor any of their employees, makes any warranty, express or implied, or assumes any legal responsibility for the accuracy, completeness, or usefulness of any information, apparatus, product, or process disclosed, or represents that its use would not infringe privately owned rights. Reference herein to any specific commercial product, process, or service by its trade name, trademark, manufacturer, or otherwise, does not necessarily constitute or imply its endorsement, recommendation, or favoring by the United States Government or any agency thereof, or the Regents of the University of California. The views and opinions of authors expressed herein do not necessarily state or reflect those of the United States Government or any agency thereof or the Regents of the University of California.

Assessment of occupant-behavior-based indoor air quality and its impacts on human exposure risk: A case study based on the wildfires in Northern California

Na Luo^{1,2,3}, Wenguo Weng^{1,2*}, Xiaoyu Xu^{1,2}, Tianzhen Hong³, Ming Fu⁴, Kaiyu Sun³

¹ Institute of Public Safety Research, Department of Engineering Physics, Tsinghua University, Beijing, 100084, P.R. China

² Beijing Key Laboratory of City Integrated Emergency Response Science, Tsinghua University, Beijing, 100084, China.

³ Building Technology and Urban Systems Division, Lawrence Berkeley National Laboratory, USA

⁴ Hefei Institute for Public Safety Research, Tsinghua University, Hefei, Anhui Province, 320601, China.

Abstract: The recent wildfires in California, U.S., have caused not only significant losses to human life and property, but also serious environmental and health issues. Ambient air pollution from combustion during the fires could increase indoor exposure risks to toxic gases and particles, further exacerbating respiratory conditions. This work aims at addressing existing knowledge gaps in understanding how indoor air quality is affected by outdoor air pollutants during wildfires—by taking into account occupant behaviors (e.g., movement, operation of windows and air-conditioning) which strongly influence building performance and occupant comfort. A novel modeling framework was developed to simulate the indoor exposure risks considering the impact of occupant behaviours by integrating building energy and occupant behaviour modeling with computational fluid dynamics simulation. Occupant behaviors were found to exert significant

*Correspondence and requests for materials should be addressed to Prof. Weng (email: wgweng@tsinghua.edu.cn)

impacts on indoor air flow patterns and pollutant concentrations, based on which, certain behaviors are recommended during wildfires. Further, the actual respiratory injury level under such outdoor conditions was predicted. The modeling framework and the findings enable a deeper understanding of the actual health impacts of wildfires, as well as informing strategies for mitigating occupant health risk during wildfires.

Key words: human exposure risk, indoor air quality, occupant behavior, respiratory injury, NAPA wildfire, computational fluid dynamics simulation

1 Introduction

2 Climate change is influencing large wildfire frequency and globally widespread disturbance that
3 affect both human and natural systems (Hurteau et al. 2014). The 2013 Rim Fire in California has
4 caused an average PM_{2.5} concentration of 20 µg/m³ and ranged from 0 to 450 µg/m³, which was
5 proved to exert significant adverse health effects to a large population (Navarro et al. 2016). As
6 another one of the worst wildfires recently, several massive wildfires swept Napa and Sonoma
7 counties in the North Bay areas of San Francisco on the western coast of the United States on the
8 night of October 8, 2017 (HST). The fires resulted in the worst air quality that has ever been
9 recorded in the San Francisco Bay Area¹. The outdoor air quality index^{2,3}, measured in particulate
10 matter (e.g., PM_{2.5}) exceeded 250 ug/m³, and a measure of other criteria pollutants⁴ (e.g., sulfur
11 dioxide – SO₂) exceeded 200 ppb, indicating that the high level of air pollution could cause serious
12 health effects in most people who breathed in the contaminated air outdoors.

13 A sudden increase in the number of hospitalizations during the days following the fires could be
14 related to the negative health effects of high gaseous and particulate pollutant levels in the area,
15 which included increased risk for asthma, and deterioration of pre-existing respiratory diseases
16 (Lewis et al. 2013). A number of recent researches reported effects of the different airborne particle
17 metrics on respiratory diseases, cardiovascular effects, lung cancer, asthma, and lung cancer via
18 human inhalation exposure (You et al. 2017; Haikerwal et al. 2015; Haddrell et al. 2015). In other
19 words, during the past decades, wildfires have exerted a large negative global impact on human

¹ Xinhua. Massive wildfires engulf north San Francisco counties. http://news.xinhuanet.com/english/2017-10/10/c_136667925.htm Accessed 2017-10-10

² EPA USA. Air Data: Air Quality Data Collected at Outdoor Monitors Across the US. <https://www.epa.gov/outdoor-air-quality-data> Accessed 2018-06-15

³ Air Quality Data Query Tool. <https://www.arb.ca.gov/aqmis2/aqdselect.php> Accessed 2018-06-15

⁴ The criteria pollutants (also known as “criteria air contaminants – CAC”) are a set of air pollutants (normally six common pollutants, which are ozone, particulate matter, carbon monoxide, lead, sulfur dioxide, and nitrogen dioxide) that cause smog, acid rain and other health hazards.

20 health, ecosystems, societies, economies and climate(Jolly et al. 2015; Jaffe et al. 2013). Even
21 worse, according to the California’s Fourth Climate Change Assessment Report (Bedsworth et al.
22 2018), there is no sign of abating in the expansion of wildfires due to the climate variations. There
23 is an urgent need to mitigate the impacts of the adverse air quality on the human health caused by
24 the increasing wildfires (Anderson et al. 2018; West et al. 2013).

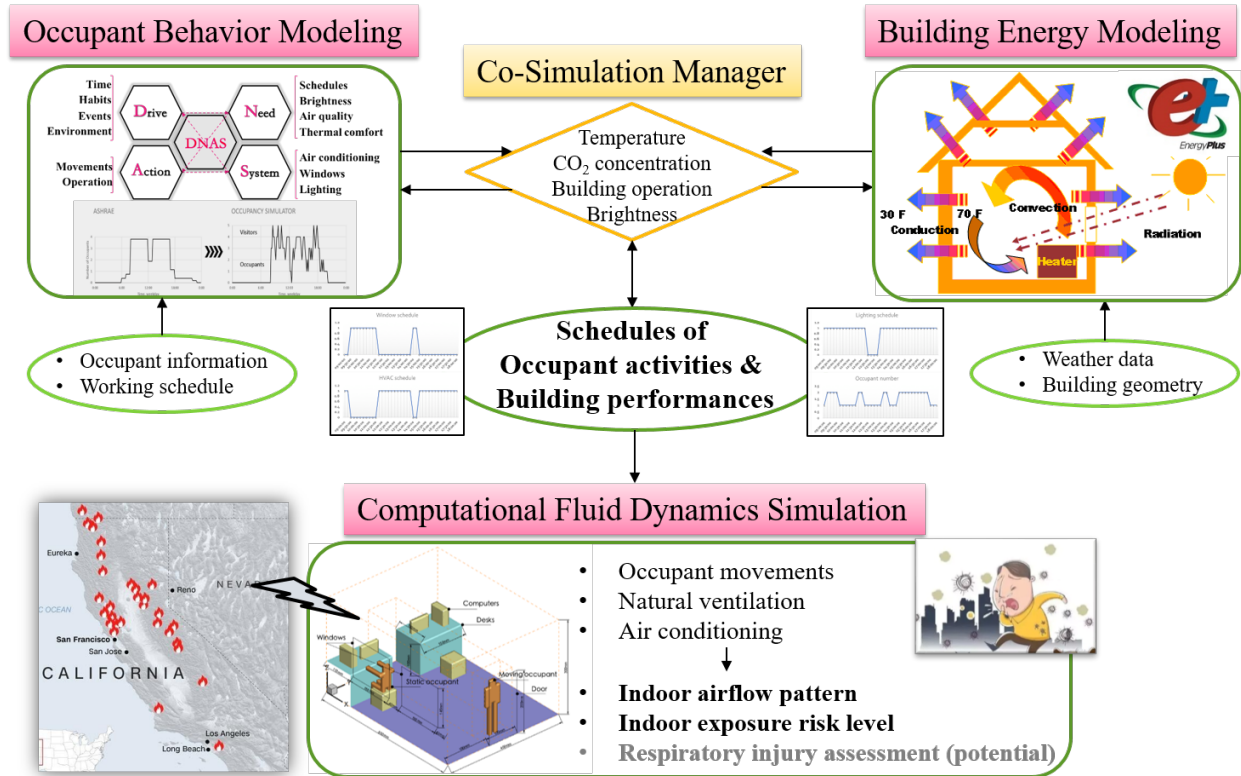
25 Since individuals spend an average of 87% of their time indoors (Klepeis et al. 2001), indoor
26 air quality (IAQ) is probably more indicative of the pollution exposure levels affecting residents’
27 health than the outdoor measures. According to the report by the Institute of Medicine (2011), IAQ
28 is affected by three main factors: occupant behavior (OB), building characteristics, and pollutant
29 properties. Among them, as the most significant factor, OB affects IAQ through occupants’
30 interactions with the outdoor physical environment. Behaviours such as window opening and
31 closing (Stabile et al. 2017), HVAC operation, and walking into or out of a room (Montgomery et
32 al. 2015) will change the boundary conditions of the indoor environment, thus influence the flow
33 pattern of indoor air, which, ultimately cause the increase or decrease of the indoor pollution levels.

34 Many previous experimental studies focused on the separate impacts of occupant behaviors and
35 building performances on the indoor airflow patterns and pollutant diffusion process, such as
36 human movements, air-conditioning system-related parameters and window operation-related
37 natural ventilation (Luo et al. 2016; Luongo et al. 2016). Several Computational Fluid Dynamics
38 (CFD) models have also been improved by validating with quantitative measurements (Luo et al.
39 2018b; Gosselin and Chen 2008). These investigations revealed detailed information about indoor
40 air flow patterns and pollutant concentration levels under different specific conditions. However,
41 in a real office environment, occupant behaviors are always complex and dynamic due to transient
42 indoor conditions such as temperature, humidity, and occupant counts, which are mostly associated

43 with the outdoor environment (Lin et al. 2017). Also, when assessing the impacts of the indoor
44 environment on human health, exposure to air pollution is not only largely determined by pollutant
45 concentrations in the spaces where people spend their time, but also by the amount of time they
46 spend in those spaces. Therefore, the static status of the indoor environment is no longer suitable
47 and appropriate for evaluating the indoor human exposure risks during daily working hours; a set
48 of OB-related dynamic schedules should be first generated to guide the indoor CFD modeling and
49 risk evaluation. Furthermore, for a given indoor environment, the respiratory injury level is also
50 crucial for assessing adverse health impacts of wildfires, which requires the pollutant concentration
51 near the oro-nasal as the boundary condition for assessment. PM_{2.5} and ultrafine particles are both
52 considered as the representative pollutants when indicating the indoor air quality level to the public
53 (Ibald-Mulli et al. 2002; Zhao et al. 2009). Several studies recognized that PM_{2.5} are better related
54 to resuspension phenomena and combustion processes, while quite a high amount of our overall
55 daily dose of ultrafine particles is due to the indoor sources. Considering the access to the measured
56 data for further validation, we selected PM_{2.5} as the main particle metrics in this work.

57 Here we used both EnergyPlus and Fluent to co-simulate indoor occupant behaviors as well as
58 the corresponding IAQ and particle deposition inside respiratory systems, respectively. Indoor
59 pollutant concentrations were simulated and used to calculate the IAQ index, which indicated
60 potential adverse health effects. Results of the properties affected by particle concentrations near
61 the mouth and nose of occupants, could be potentially used as the initial and boundary conditions
62 for the assessment of the respiratory injury. Outcomes from the study formulated a framework for
63 modeling (as shown in Figure 1) exposure to indoor pollutants as well as the potential assessment
64 of human health hazards in an office environment—considering occupant movement and behavior,
65 which can inform strategies to mitigate occupant health issues during times of serious outdoor air

66 pollution such as wildfires. For broader application, this co-simulation framework among Building
 67 Energy Modeling (BEM), occupant behavior modeling and CFD builds a bridge in the outdoor-
 68 to-indoor penetration process especially considering the indoor occupant behaviors, which thus
 69 could be broadly applied in the assessment of indoor quality under many other extreme weather
 70 events or use cases such as haze pollution in China, as well as the vehicle exhaust etc.



71

72 **Figure 1 Overview of the modeling framework.** The Building Energy Modeling tool (EnergyPlus)
 73 was co-simulated with the Occupant Behavior Modeling tool (obFMU – a functional mockup unit of
 74 occupant behavior model) to calculate the occupant-related schedules, primarily based on the outdoor
 75 environment and the building performance. These modeled activities and building performances were then
 76 integrated into the Fluent modeling process as the boundary conditions through a C++ user-defined function
 77 (UDF), to further calculate the indoor airflow and contaminant concentration. Eventually, the corresponding
 78 indoor exposure risk could be evaluated, as well as the respiratory injury level as one of the potential
 79 assessments in the future work.

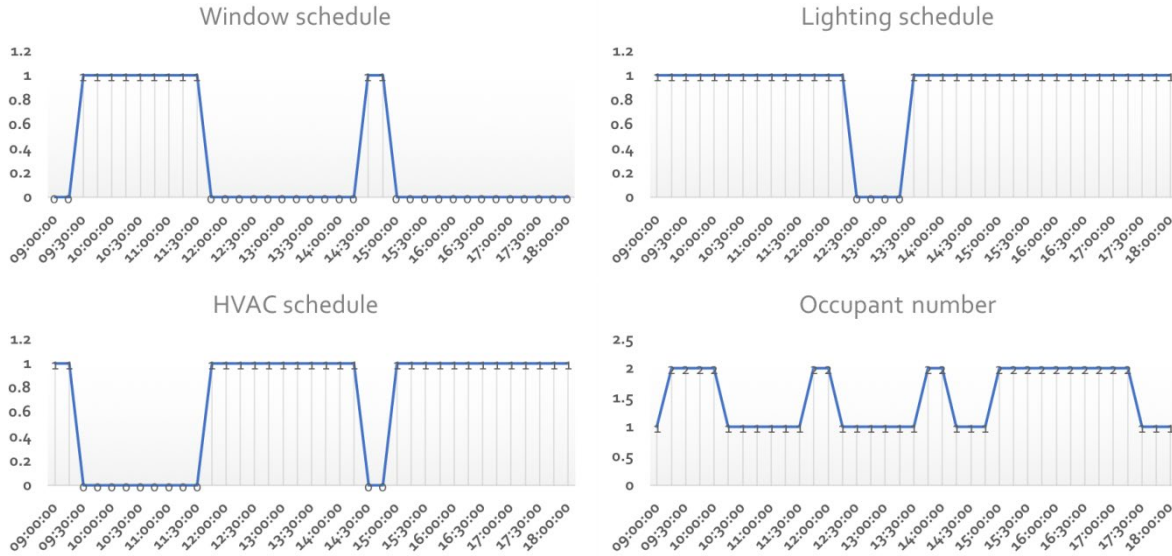
80

81 **Materials and Methods**

82 **Occupant behavior modeling.** Whole building performance simulation, using EnergyPlus
83 coupled with obFMU, has been used to simulate occupant behavior and generate occupant-related
84 schedules in the last decade (Hong et al. 2017). EnergyPlus is an open-source program that models
85 heating, ventilation, cooling, lighting, water use, renewable energy generation, and other building
86 energy flows (Crawley et al. 2001). It is the flagship building simulation engine supported by the
87 United States Department of Energy (DOE). The occupant behavior function mockup unit
88 (obFMU) is an occupant behavior-modeling tool developed by Lawrence Berkeley National
89 Laboratory (T. Hong et al. 2016). It was developed for co-simulation with EnergyPlus, requiring
90 an XML file generated based on the obXML (occupant behavior eXtensible Markup Language)
91 schema (Hong, D'Oca, Taylor-Lange, et al. 2015) and a configuration file. The obXML schema
92 describes the occupant behavior by implementing a DNAS (drivers-needs-actions-systems)
93 framework (Hong, D'Oca, Turner, et al. 2015). The obFMU is the engine for occupant behavior
94 simulation and co-simulates via the functional mockup interface (FMI) with building performance
95 simulation programs, e.g., EnergyPlus and ESP-r.

96 **Occupant behavior activities.** In this work, the simulated scenario is designed in an office room
97 with two occupants working as different types. One occupant keeps working on the computer,
98 while the other works as a secretary, who might often walk out of the room to get printed materials
99 or coordinate with other people. The simulation period is from 9:00am to 6:00pm, which are the
100 working hours for the office workers. According to the weather data on October 13, 2017, the
101 building performance, including the four occupant-related schedules and the operation
102 characteristics of the indoor facilities, were modeled in EnergyPlus. Four categories of occupant
103 behavior models were used in this study: occupant movement, lighting, windows, and HVAC
104 operation. They were used to describe the characteristics of related occupant behaviors, based on

105 which the probability of occupants taking an action is estimated. More specifically, Chen’s agent-
106 based stochastic occupant movement model (Chen et al. 2018), Haldi’s lighting control models
107 (switch on light at arrival or when it is dark, switch off at departure) (Haldi 2013), and Newsham’s
108 window control model (open at arrival or when the outdoor environment is suitable, close at arrival,
109 departure or when the outdoor environment is not suitable) (Newsham 1994) were adopted. HVAC
110 operation is a combination of availability schedule and actual window operation. In other words,
111 when the window is open, the HVAC system will be off; when the window is closed, the HVAC
112 system will be on if occupants feel hot. The occupant behavior models were compiled in an
113 obXML file, which worked as the input to obFMU and was used to co-simulate with EnergyPlus.
114 Occupant-related schedules, including the occupancy schedule, lighting schedule, natural
115 ventilation schedule (namely window schedule), as well as the HVAC schedule were generated in
116 the simulation process, seen in Figure 2. As for the detailed characteristics, the operation
117 parameters of the windows and HVAC refer to the velocity, temperature, and pollutant
118 concentration of the inlet airflow. The electric power of the lighting and computers was associated
119 with the indoor environment in the modeling process. The changes of occupant count represented
120 the moments when the occupant was entering or leaving the room.



121

122 **Figure 2. Four occupant-related schedules from the co-simulation of EnergyPlus and**
 123 **obFMU.**

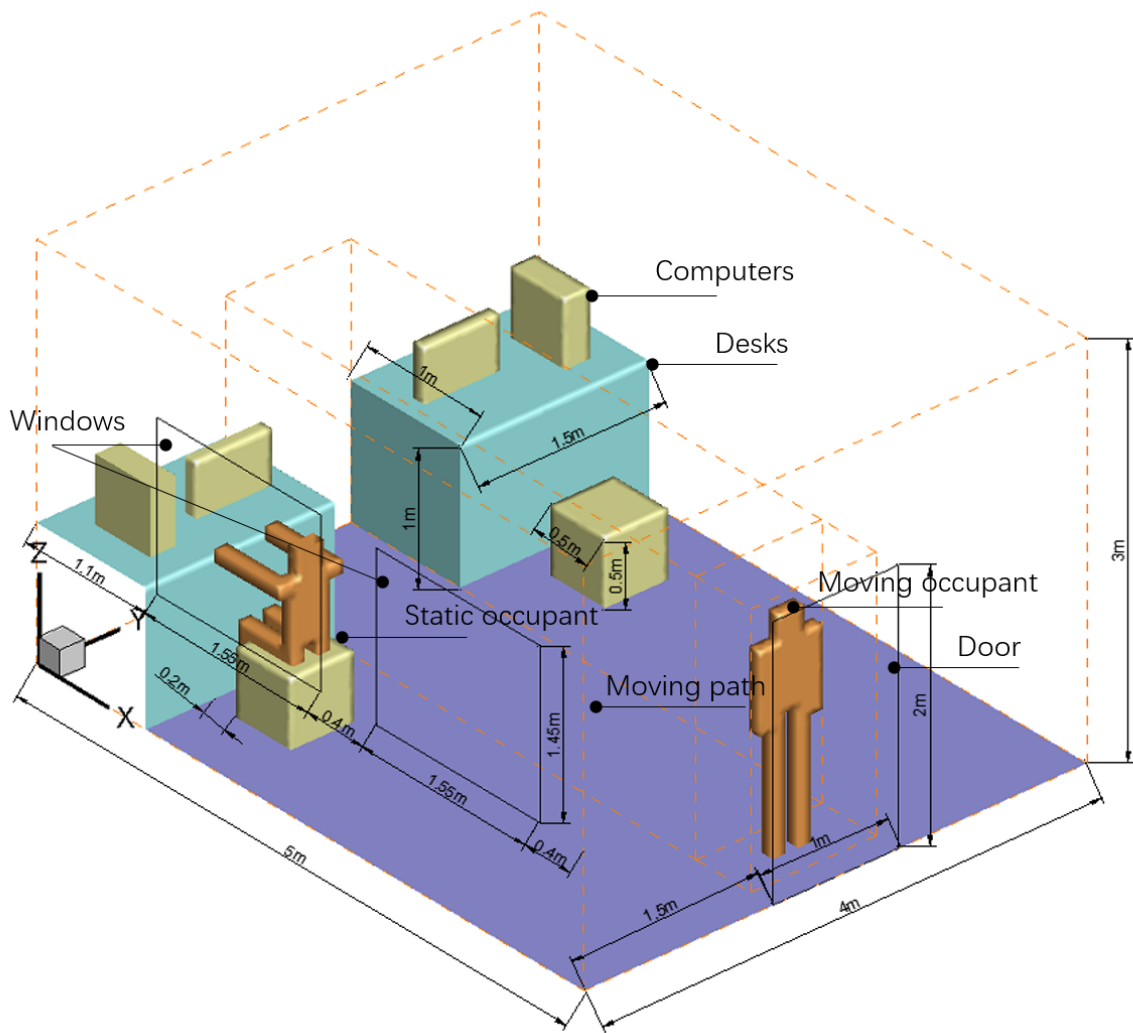
124 **Indoor air flow field modeling.** The CFD software ANSYS Fluent (Version 18.0.0) was
 125 employed to simulate the transient indoor flow field affected by the occupant behaviors. Gambit
 126 (Version 2.4.6) was used to build the geometric model of the office room (Figure 3) and generate
 127 the grids for simulation. The total number of grids is 6.7 million. The minimum mesh volume was
 128 $2.64 \times 10^{-9} \text{m}^3$, located close to the skin of the moving occupant. The method of mesh generation
 129 was used in our previous study (Luo et al. 2018a, 2018b). The transient solver was employed
 130 during the calculation. As for representing the turbulence airflow caused by the ventilation and
 131 occupant movements, the RNG k- ϵ model adopted in this work was validated by previous work
 132 (Zhang et al. 2009; Han et al. 2014; Fracastoro et al. 2002), with the overall consideration of
 133 accuracy, computing efficiency, and affordability for modeling the indoor flow field. The
 134 differential viscosity model and the swirl dominated flow in the RNG options were selected.
 135 During the iterative process, the pressure-implicit with splitting of operators (PISO) algorithm was
 136 employed to solve the pressure-velocity coupling equations. The second-order upwind scheme was
 137 also used to consider the diffusion-convection in the governing equation. The Discrete Element

138 Model (DEM) Collision term and the Brownian Motion term were both applied to include the
 139 particle-particle interactions (voidage and collision), which captured the particle resuspension
 140 phenomenon of PM2.5. According to the aforementioned schedules and the related parameters, a
 141 UDF in the Fluent software has been created to automate the transient changes of the window
 142 boundary conditions, HVAC boundary conditions, light conditions, and the human movement
 143 status. The gaseous composition and the corresponding concentrations of the inlet airflow were
 144 based on the measured outdoor air quality data, seen in Table 1. The time steps during the occupant
 145 moving and static process were set to 0.01 s and 1 s, respectively. The calculation is computed in
 146 a four-node Linux cluster. Each node of the cluster has 12 processors (2.4 GHz Intel 64). The
 147 overall simulation period in this case is nine hours (32400 seconds), which requires 120 hours of
 148 the computing time.

149 **Table 1. The daily maximum outdoor air quality of some criteria pollutants (SO₂, CO, and**
 150 **O₃) and the particulate matter (PM2.5) within the following week after the wildfire event in**
 151 **Northern California (October 8 – 14, 2017).** The gaseous composition and the corresponding
 152 concentrations of the inlet airflow was based on the measured outdoor air quality data.

	Oct. 8	Oct. 9	Oct. 10	Oct. 11	Oct. 12	Oct. 13	Oct. 14
SO ₂ (ppb)	65.90	89.49	/	/	248.93	439.05	345.92
CO (ppm)	0.80	1.19	/	1.29	1.83	2.84	2.29
O ₃ (ppb)	12.72	25.49	31.40	33.54	76.57	92.08	50.48
PM2.5 (ug/m ³)	86.30	115.30	214.70	/	91.97	212.49	179.40

153



154
 155 **Figure 3. The geometrical features of the office room.** There are two desks (1.0 m × 0.5m × 0.7
 156 m in length × width × height) at one side of the room (5 m × 4 m × 3 m in length × width × height).
 157 One occupant remains sitting in front of the desk, the other one (1.75 m-height) walks through the
 158 door (2 m × 1 m in height × width), which is on the other side of the room. There are two windows
 159 (1.55 m × 1.45 m in width × height) on the side wall, which is adjacent to the seated occupant. The
 160 diffuser outlet of the HVAC (0.3 m × 0.2 m in width × height) is at the top of the wall towards the
 161 door. The lighting fixture is at the center of the ceiling.

162
 163 **UDF setting.** The UDF (user-defined function) setting is a very important link in the overall
 164 framework, serving as a “bridge” connecting the outdoor and indoor concentration conditions, as
 165 well as taking the occupant behavior into consideration. The aforementioned generated occupant-
 166 related schedules determined both the natural and mechanical ventilation strategies (such as

167 opening and closing time, as well as the air flow rate and its temperature etc.), these strategies
168 were implemented in the CFD simulation as “time-series data” through coding the user-defined
169 function. The natural ventilation strategy in Newsham’s research (Newsham 1994) is adopted in
170 this work (open at arrival or when the outdoor environment is suitable, close at arrival, departure
171 or when the outdoor environment is not suitable). Thus, when the windows were opened, the
172 gaseous and particulate pollutants were blown into the room through the windows and the doors,
173 where the velocity and temperature of the inlet airflow were set as the EnergyPlus modeling results.
174 As for the mechanical ventilation strategy, it is a combination of availability schedule and actual
175 window operation (when the window is open, the HVAC system will be off; when the window is
176 closed, the HVAC system will be on if occupants feel hot). While the HVAC system was on, the
177 windows and the door, as well as the outdoor air system of the HVAC system, were all considered
178 to be closed. The air purification system was assumed to be active in this work, with a removal
179 rate of 50%. Thus, the gaseous composition and the corresponding concentrations of the next
180 timestep’s inlet airflow were calculated and input in the UDF code, according to the 50%
181 concentration of reduced pollutants of the last timestep around the HVAC outlet. The air
182 temperature and velocity of the inlet airflow were also set using the EnergyPlus modeling results.
183 As for the movement behavior, the walking speed of the occupant was set to 1 m/s, and it took 5 s
184 walking from the door to his seat (same in the opposite direction).

185 **Calculation of IAQ index.** The IAQ index is an index developed by the United States
186 Environmental Protection Agency (EPA) that is used to indicate the indoor air quality in terms of
187 its adverse health effects. On one side, the pollutant concentrations can be converted into the index
188 value based on an empirical piecewise linear function. The breakpoints of specific pollutants are
189 guided in the reports released by WHO in 2005 and 2010 (World Health Organization 2005; 2010).

190 On the other side, the calculated index values are corresponding to different levels of adverse
191 health symptoms based on many previous epidemiological studies and surveys. The IAQ index for
192 each pollutant can be calculated from the modeled pollutant concentration results, as shown in Eq.
193 1.

$$194 \quad I_P = \frac{I_{Hi} - I_{Lo}}{BP_{Hi} - BP_{Lo}}(C_P - BP_{Lo}) + I_{Lo} \quad (1)$$

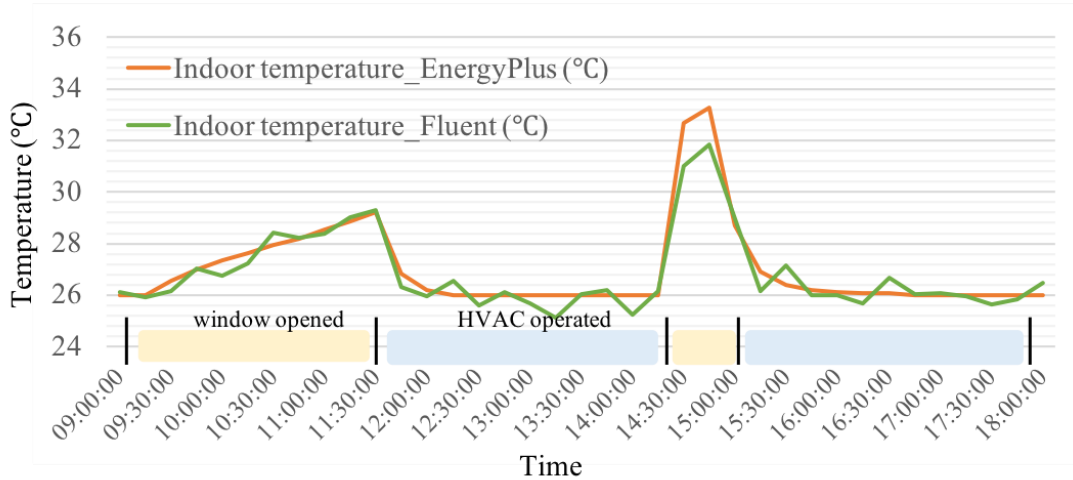
195 where I_P is the index for pollutant P , C_P is the rounded concentration of pollutant P , BP_{Hi} is
196 the breakpoint that is greater than or equal to C_P , BP_{Lo} is the breakpoint that is less than or equal
197 to C_P , I_{Hi} is the AQI value corresponding to BP_{Hi} , and I_{Lo} is the AQI value corresponding to
198 BP_{Lo} . According to the aforementioned concentration distribution, the average potential inhaled
199 concentration was calculated within the vertical plane in front of the static human. The
200 corresponding air quality level was then calculated based on Eq. 1. While the final AQI is the
201 highest value calculated for each pollutant (Shi et al. 2015).

202

203 **Results**

204 **Verification of the consistency of the two simulations.** It was assumed that the occupant-related
205 schedules remained the same in the two simulated environments of EnergyPlus and Fluent, making
206 the process consistent. Due to the model that we employed in the obFMU, decision making
207 regarding the operations of windows and HVAC was largely dependent on the indoor environment,
208 especially room air temperature. Thus, to verify the consistency of the two simulated
209 environments, indoor average temperature was chosen as the parameter for comparison. Figure 4
210 shows the indoor temperature modeled in EnergyPlus and Fluent, respectively. The occupant-

211 related schedules generated in EnergyPlus were proved to be reasonable for the indoor
212 environment simulated in Fluent.



213

214 **Figure 4. The indoor temperature simulated in EnergyPlus and Fluent.** For EnergyPlus and
215 Fluent simulations, indoor temperature both rose slowly till around 29.2 °C before 11:30 am,
216 when the windows were opened. Then, the temperature remained at around 26.0 °C until 2:30 pm
217 within the duration when the HVAC was turned on. The same phenomenon appeared for such
218 behaviours afterward. Thus, the occupant-related schedules generated in EnergyPlus were
219 reasonable for the indoor environment simulated in Fluent.

220

221 **IAQ from measured data and simulated results.** The indoor and outdoor air qualities before and

222 after this wildfire event were provided by the Indoor Environment Group at Lawrence Berkeley

223 National Laboratory (LBNL). Some office rooms inside the Building 51F in Lawrence Berkeley

224 National Laboratory (LBNL) are serving as a living laboratory to continually monitor the indoor

225 and outdoor carbon dioxide and pollutant concentrations (e.g., ozone, particular matters). Figures

226 5-6 show the comparisons of IAQ level (namely ozone and PM2.5) between the measured and

227 simulated results. Since more detailed IAQ measurement was not available, we chose the average

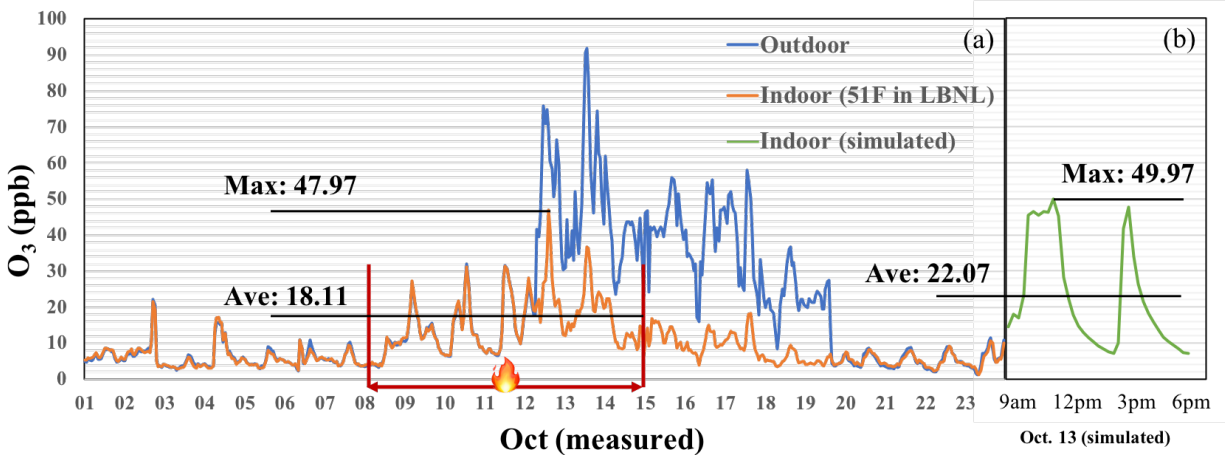
228 and maximum concentration levels as the comparison indexes of the measured and simulated

229 results. From Oct. 8 to Oct. 15, 2017, IAQ worsened after the breakout of the wildfire, and

230 continued for the next whole week (Figure 5 (a)). During this week, the average concentration

231 level of the indoor ozone was 18.11 ppb. The maximum levels of the ozone reached 47.97 ppb on

232 October 12, 2017, when the outdoor quality data was 76 ppb. The simulated average and maximum
 233 levels of ozone in Figure 5 (b) were overall consistent with the measured results, except for two
 234 details. First, ozone is a highly reactive component that reacts quickly with surfaces when
 235 penetrating indoors, which is why the measured ozone levels are generally lower than those
 236 modeled levels. Second, the measured indoor ozone level stayed at 10 ppb during the night when
 237 all unintentional openings of the building were closed, during which time, the simulated result was
 238 almost zero. These differences between the measured and modeled results were supposed to be
 239 associated with air infiltration in the building and are further discussed in the discussion section.
 240

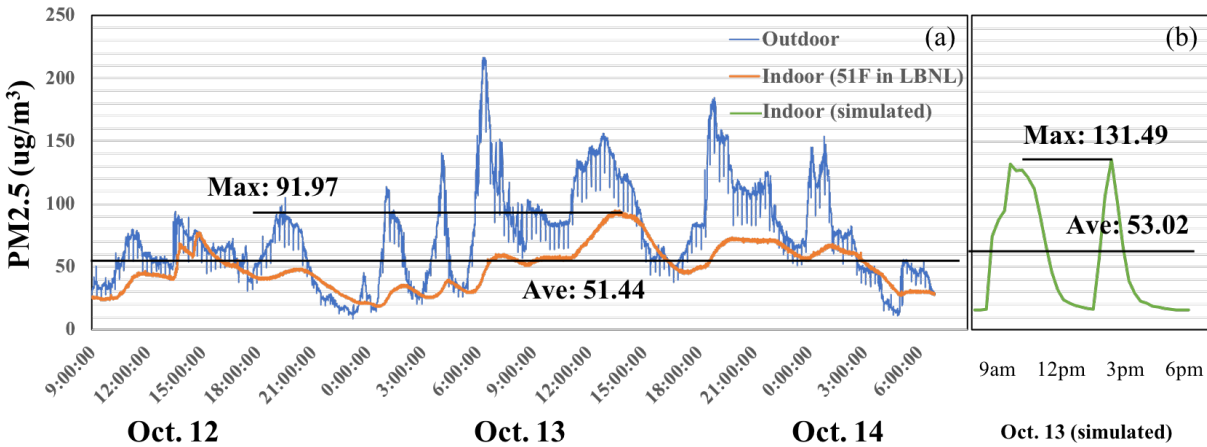


241
 242 **Figure 5 Comparison of the measured and simulated O₃ levels.** (a) Concentration of Ozone
 243 measured indoors and outdoors, before, during and after the wildfire. (b) The simulated concentration of
 244 the indoor Ozone on Oct. 13.
 245

246 Measured data of particle levels from October 12 to 14 indicate that the maximum and average
 247 levels of PM_{2.5} were 91.97 ug/m³ and 51.44 ug/m³, respectively (Figure 6 (a)), while those of the
 248 simulated results were 131.49 ug/m³ and 53.02 ug/m³, respectively (Figure 6 (b)). The simulated
 249 results were a little higher than the measured data, which might be due to less consideration of the

250 particle interaction. Comparing to the outdoor concentration, the indoor PM was about 65% of the
251 outdoor level on average, under an air exchange rate of 0.7 air changes per hour in this work.

252



253

254 **Figure 6 Comparison of the measured and simulated PM2.5 levels.** (a) Concentration of PM2.5
255 measured indoors and outdoors during the wildfire. (b) The simulated concentration of the indoor PM2.5
256 on Oct. 13.

257

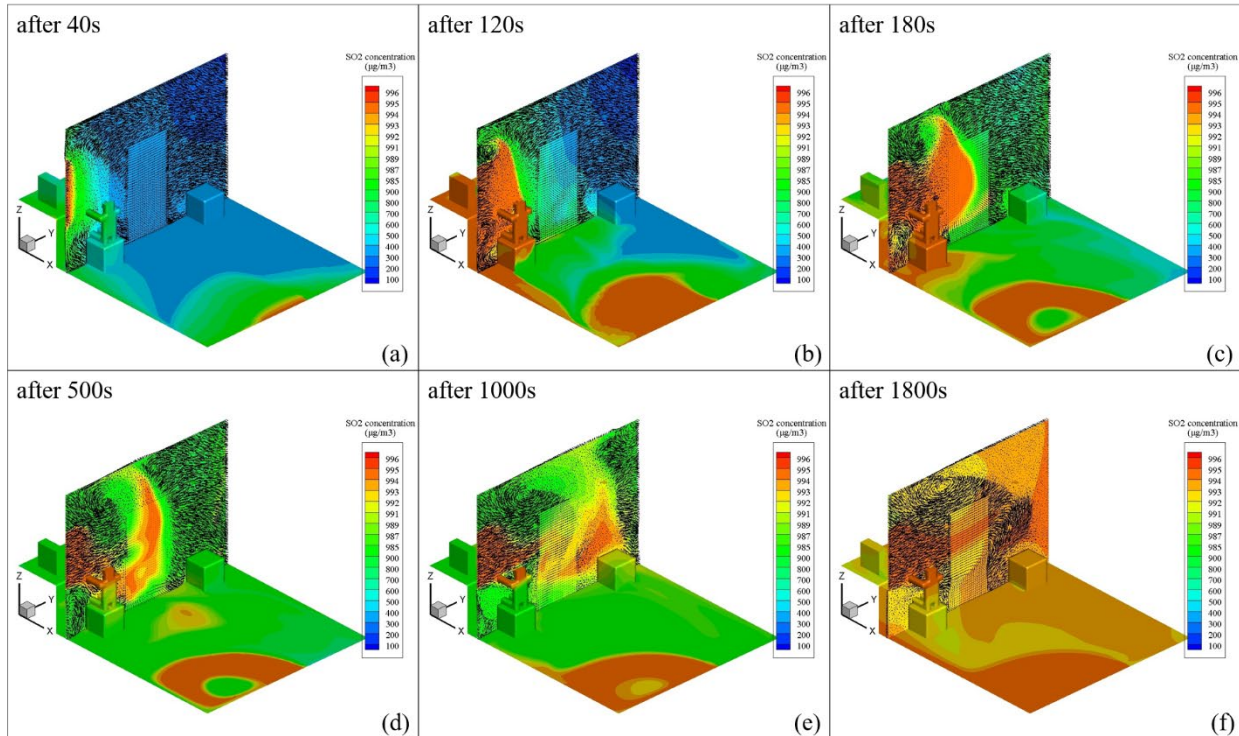
258 The fluctuant simulated results indicated that occupant behaviors exerted a large influence on
259 the indoor pollutant concentration during the working hours. Through the comparison, the
260 fluctuant indoor concentration level was proved to be consistent with the measured data in the
261 actual office environment if the occupant behaviors were considered during the simulation.

262

263 **Flow pattern and concentration distribution.** The plane in front of the oronasal ($x=1.25\text{m}$, see
264 Figure 3) region was chosen as the potential inhalation region. The evolution of the flow structure
265 and the concentrations of different gaseous pollutants in this region may largely influence human
266 inhalation doses, which is significant in assessing exposure risk levels. According to the
267 aforementioned outdoor air quality on that day, the outdoor concentration of sulfur dioxide (SO_2)
268 was much higher than an average day, and its hazard level was higher than that of carbon monoxide

269 and ozone. Thus, sulfur dioxide was chosen as the representative pollutant to investigate its
270 diffusion characteristics.

271



272

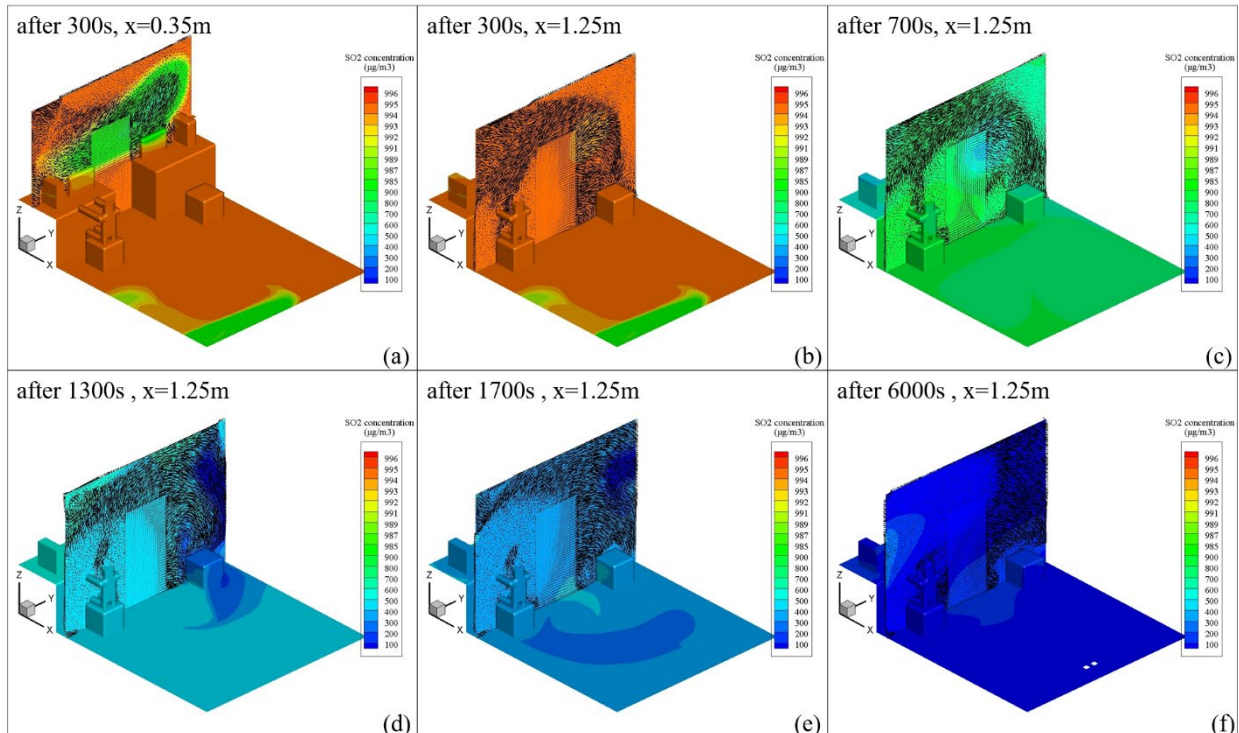
273 **Figure 7 The velocity and concentration fields of SO₂ indoors after the windows were opened.**
274 (a) At inhalation plane, 40s after the window was opened. (b) After 120s. (c) After 180s. (d) After 500s.
275 (e) After 1000s. (f) After 1800s.

276

277 Operation of windows exerted a significant impact on flow pattern and concentration
278 distribution (Figure 7). Outdoor sulfur dioxide was diffused quickly through the windows. Owing
279 to the short distance between the seated occupant and the windows, the concentration of the sulfur
280 dioxide near the oro-nasal region reached a relatively high level just after 120s (Figure 7 (b)). The
281 inlet airflow was affected by transient outdoor weather data, such as wind velocity and direction
282 outdoors. Meanwhile, the diffusion of the inlet airflow was also influenced by the existent indoor
283 airflow circulation. Eventually, the concentration of sulfur dioxide remained at a steady state after

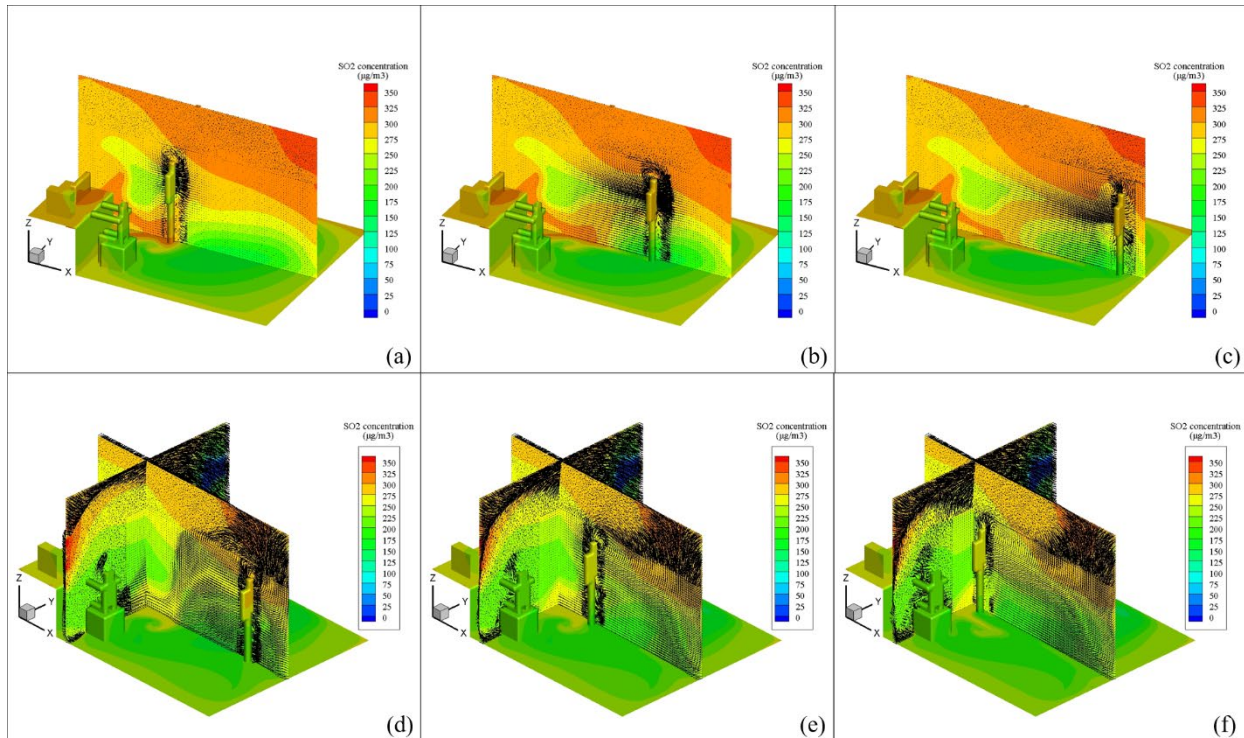
284 30 min, which was around 995 ug/m^3 (348.25 ppb). Due to the same pattern of the velocity field,
285 concentration evolutions for carbon monoxide and ozone were similar to that of the sulfur dioxide.
286 Eventually, after 30 min of opening the windows, concentrations of indoor carbon monoxide and
287 ozone on the inhalation region ($x=1.25 \text{ m}$) reached around 1.40 mg/m^3 (1.12 ppm) and 107.08
288 ug/m^3 (49.97 ppb), respectively.

289 Flow pattern and concentration distribution caused by other occupant behaviors such as air-
290 conditioning and movement can be found in Figure 8-9. The velocity and concentration fields on
291 the plane near the HVAC outlet 300 s after the HVAC was turned on, indicated the effects of the
292 HVAC operation on the IAQ (Figure 8 (a)). The cold air coming from the HVAC outlet moved
293 downwards during the diffusion (Figure 8 (b-f)). 1300 s after the HVAC operation, the
294 concentration of indoor sulfur dioxide dropped to 500 ug/m^3 . And 6000 s after the HVAC operation,
295 the concentration of sulfur dioxide remained at a relatively steady state, which was around 100
296 ug/m^3 . Combined with the aforementioned analysis, occupants are advised to keep the windows
297 closed and run the HVAC systems with the outdoor air dampers shutting off during wildfire to
298 mitigate the indoor exposure risk.



299 **Figure 8** The velocity and concentration fields of SO₂ indoors after the HVAC was turned
 300 **on.** (a) At the plane near the HVAC outlet, 300 s after the HVAC was operated. (b) At inhalation
 301 plane, 300 s after the HVAC was operated. (c) After 700 s. (d) After 1300 s. (e) After 1700 s. (f)
 302 After 6000 s.
 303
 304

305 The effects of the occupant movements, i.e. walking out of and into the room, can be found in
 306 Figure 9 (a-c) and (d-f), respectively. A strong downward airflow was observed behind its upper
 307 body, carrying the gaseous pollutant downwards; while the gap between the lower limbs exerted a
 308 horizontal flow between the legs, which enhanced the diffusion speed of the pollutants. The
 309 detailed information of the velocity fields evaluated in this study has been verified in a previous
 310 PIV experimental study (Luo et al. 2018a). Overall, the movement behavior accelerated the
 311 diffusion and mixture of the existed contaminants at different heights, which enhanced the risk of
 312 respiratory exposure. Therefore, occupants are recommended to limit walking activities during the
 313 extreme wildfires.



314 **Figure 10 The velocity and concentration fields of SO₂ along the moving.** (a-c) The occupant
 315 was walking out of the office. (d-f) The occupant was walking into the room.
 316
 317

318 **Assessment of the daily exposure risk level.** Epidemiological studies have linked exposure to
 319 indoor air pollution with a wide range of adverse health outcomes. The health effects and the
 320 breakpoints of some specific pollutants considered in this study are listed in Table 2 (documented
 321 from (WHO 2010; Mintz 2013; World Health Organization 2005)).

322 **Table 2. Pollutant-specific sub-indices and health effects statements for guidance on the AQI.**
 323 The IAQ index for each pollutant can be calculated from the modeled pollutant concentration
 324 results, seen in Methods.

AQI Categories: Index Values	Ozone (ppb)		Sulfur Dioxide (ppb)		Carbon Monoxide (ppm) [8-hour]	Particulate Matter (ug/m ³) [24-hour]
	[1-hour]	[8-hour]	[1-hour]	[24-hour]		
Good (Up to 50)	-	0-59 None	0-35	0-30	0-4.4 None	0-12.0 None
Moderate (51-100)	-	60-75 Unusually sensitive individuals may experience respiratory symptoms	36-75	>30-140	4.4-9.4 None	12.1-35.4 Respiratory symptoms possible in unusually sensitive individuals; possible aggravation of heart or lung disease in people with cardiopulmonary disease and older adults
			None			

Unhealthy for Sensitive Groups (101-150)	125-164	76-95	76-185	140-220	9.5-12.4 Increasing likelihood of reduced exercise tolerance due to increased cardiovascular symptoms, such as chest pain, in people with heart disease	35.5-55.4 Increasing likelihood or respiratory symptoms in sensitive individuals; aggravation of heart or lung disease and premature mortality in people with cardiopulmonary disease, older adults, and people of lower SES
	Increasing likelihood of respiratory symptoms and breathing discomfort in people with lung disease, such as asthma, children, older adults, and outdoor workers		Increasing likelihood of respiratory symptoms, such as chest tightness and breathing discomfort in people with asthma			
Unhealthy (151-200)	165-204	96-115	186-304	220-300	12.5-15.4 Reduced exercise tolerance due to increased cardiovascular symptoms, such as chest pain, in people with heart disease	55.5-150.4 Increased aggravation of heart or lung disease and premature mortality in people with cardiopulmonary disease, older adults, and people of lower SES; increased respiratory effects in general population
	Greater likelihood of respiratory symptoms and breathing difficulty in people with lung disease, such as asthma, children, older adults, and outdoor workers; possible respiratory effects in general population		Increased respiratory symptoms, such as chest tightness and wheezing in people with asthma; possible aggravation of other lung disease			
Very Unhealthy (201-300)	205-404	116-374	305-604	300-600	15.5-30.4 Significant aggravation of cardiovascular symptoms, such as chest pain, in people with heart disease	150.5-250.4 Significant aggravation of heart or lung disease and premature mortality in people with cardiopulmonary disease, older adults, and people of lower SES; significant increased respiratory effects in general population
	Increasing severe symptoms and impaired breathing likely in people with lung disease, such as asthma, children, older adults, and outdoor workers; increasing likelihood of respiratory effects in general population		Significant increase in respiratory symptoms, such as wheezing and shortness of breath, in people with asthma; aggravation of other lung diseases			
Hazardous (301-500)	405-604	-	605-1004	600-1000	30.5-50.4 Serious aggravation of cardiovascular symptoms, such as chest pain, in people with heart disease; impairment of strenuous activities in general population	250.5-500.4 Serious aggravation of heart or lung disease and premature mortality in people with cardiopulmonary disease, older adults, and people of lower SES; serious risk of respiratory effects in general population

325

326 According to the modeled concentration results, where the 1-hour SO₂ value was 348.25 ppb,
327 CO value was 1.12 ppm, the O₃ value was 47.97 ppb, and the PM_{2.5} value was 131.49 ug/m³, the
328 calculated maximum IAQ index was 215, with SO₂ as the responsible pollutant. Qualitative
329 evaluation indicated that this environment would cause an increasing likelihood of respiratory
330 symptoms, such as wheezing, chest tightness and breathing discomfort in people with asthma, as
331 well as an increasing aggravation of other lung diseases. However, to achieve the quantitative
332 evaluation of the injury level, further analyses should be conducted considering an entering path
333 of the particle and gaseous contaminants into the body through breathing. The modeled dynamic
334 indoor contaminant concentration can be served as a boundary condition.

335 As for the impact of occupant behaviors on the daily exposure risk level, due to the distribution
336 of different indoor occupant behaviors, the indoor pollutant concentration fluctuated obviously
337 during the working hours. Activities such as opening the windows as well as walking into and out
338 of the rooms led to the increase of the pollutant concentration and thus the exposure risk of the
339 human body and respiratory. While turning on the air-conditioning without the function of
340 supplying fresh air decreased the indoor contaminant concentration in a slow but effective way.
341 Therefore, to mitigate indoor exposure risk, occupants are advised to keep windows closed and
342 limit walking activities during the extreme wildfires. Meanwhile, outdoor air dampers should be
343 shutting off when operating the HVAC system to avoid more purification loads. From another
344 aspect, a proper and accurate set of occupant behavior schedules and the corresponding building
345 boundary conditions are also crucial for enhancing the evaluation and prediction of the indoor risk
346 exposure.

347 **Discussions**

348 This study formulated a framework for the indoor pollutants exposure modeling and the potential
349 human health hazard assessment in an office environment particularly taking into account the
350 actual occupant behaviours. The simulated results under this framework were compared with the
351 actual measured indoor and outdoor data (O_3 and $PM_{2.5}$), showing great consistency in both the
352 maximum and average levels. The indoor airflow pattern and IAQ fluctuated obviously within
353 working hours, which were largely dependent on specific occupant behaviors. Therefore,
354 comparing to the traditional IAQ and occupant exposure assessments when occupants remained
355 static or the indoor equipment (e.g., HVAC and windows) remained constant running, the
356 framework in this study is proved to provide a more realistic and reliable result aligned with the
357 actual requirement of assessing the health hazard level of the indoor occupants. Furthermore, based

358 on this result as a boundary condition, the deposit fraction and equation can be fitted to predict a
359 more accurate and dynamic respiratory exposure dosage under such outdoor wildfire conditions,
360 which not only indicates the key injury level, but also provides reference for the further
361 physiological stage.

362 **Assessment of the respiratory injury**

363 As aforementioned, the indoor pollutant concentration near the oro-nasal could be considered as
364 the boundary condition for assessing the respiratory deposition. Take nasal inhalation as an
365 example, respiratory injury was mainly caused by the micron particle deposition fraction in nasal
366 cavity, pharynx, larynx and trachea regions for nasal breathing. The detailed modelling method
367 and flow pattern inside the respiratory system were included in another published journal article
368 (Xu et al. 2018).

369 The simulated particle size range was slightly expanded to allow a wider coverage of the
370 developed deposition equations. For micron-sized particles, deposition fractions were related to
371 the inertial parameter I , which considered particles mass to the square power, and the averaged
372 fluid momentum. The inertial parameter is defined as:

$$373 \quad I = d_p^2 Q \quad (2)$$

374 where Q is the volume flow rate (cm^3/s) and d_p (μm) is the particle aerodynamic diameter.
375 Figure 11(a) and (c) show the deposition fraction in human respiratory airways for particles
376 ranging from $0.8 \mu\text{m}$ to $20 \mu\text{m}$ against the inertial parameter for oral and nasal inhalation,
377 respectively.

378 The Stokes number was used to correlate the deposition to length scale, particle density, size
379 and flow rate. It is defined as:

380

$$St = \frac{\rho_p d_p^2 u C_c}{18 \mu L} \quad (3)$$

381

where L is the characteristic length of oral and u is the local airflow velocity. The deposition

382

through oral breathing in human airway was related to St and Re .

383

For the deposition equation in human airway, improved fittings were obtained with $St^{3.271} Re$ and

384

$St^{1.77} Re^{0.145}$ for particle sizes from 0.8 to 20 μm , breathing rate of 10 and 30 L/min for oral and

385

nasal breathing (Figure 11(b) and (d)), with a coefficient of determination $R^2=0.99$. The empirical

386

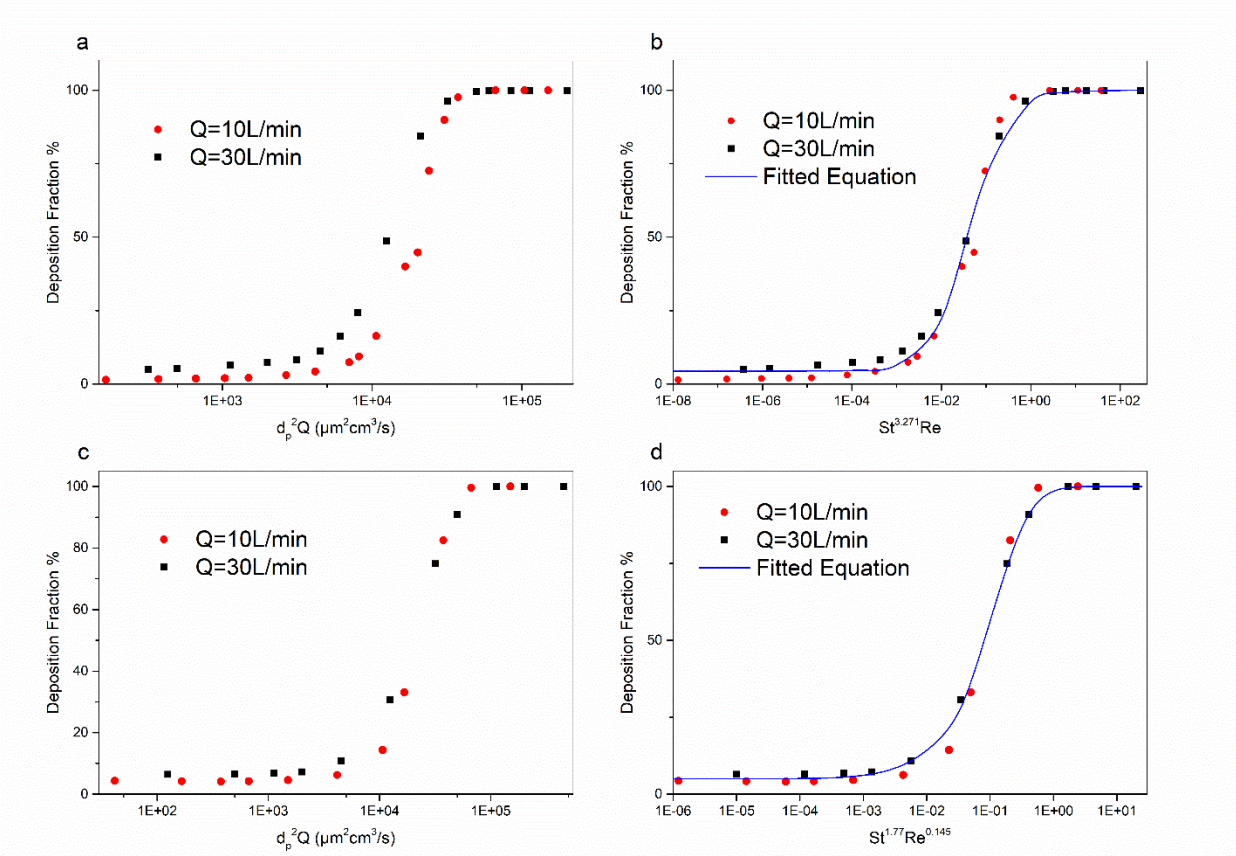
equations are given as

387

$$DF_{oral} = \left[1 - \frac{0.956}{22.701 St^{3.271} Re + 1} \right] \times 100\% \quad (4)$$

388

$$DF_{nasal} = [1 - 0.95 \exp(-7.35 \cdot St^{1.77} Re^{0.145})] \times 100\% \quad (4)$$



389

390 **Figure 11 Comparison of micron particles (0.8 – 20 μm).** (a) deposition fraction for oral
 391 inhalation. (b) fitted deposition equation for oral inhalation. (c) deposition fraction for nasal
 392 inhalation. (d) fitted deposition equation for nasal inhalation.

393

394 The dosimetry (in number, mass, surface area) in human upper airway under various breathing
 395 flow rates and breathing pattern was calculated by using the above simulated PM2.5 concentration
 396 value, presented in Table 3. The time period of occupants staying indoors was assumed as 8 hours
 397 a day (as the working hours from 9am to 5pm). A monotonous growth was obtained in human
 398 upper airway dosimetry with the flow rate, which lead to a larger air exchange and particle
 399 exposure risk, as well as a higher probability of chronic respiratory diseases.

400 **Table 3 Human upper airway dosages of indoor PM2.5 during a day.**

Q (L/min)	Oral inhalation			Nasal inhalation		
	Number (10 ⁶ #)	Mass(μg)	Surface area (10 ⁻⁵ m ²)	Number (10 ⁶ #)	Mass(μg)	Surface area (10 ⁻⁵ m ²)
10	2.93	23.96	5.75	6.41	52.16	12.60
30	36.25	296.6	71.18	31.11	255.3	61.15

401

402 **Limitations**

403 One limitation of this work is that air infiltration via building permeability (e.g., windows,
 404 envelope cracks) was not considered during the CFD simulation. Several previous studies (Shi et
 405 al. 2015; G. Hong and Kim 2016; C. Chen and Zhao 2011) have proved the effects of air infiltration
 406 on IAQ and verified the infiltration factor as the useful parameter for qualifying the number of
 407 indoor particles infiltrating from the outdoor environment. To evaluate the potential effect of
 408 building permeability on the current results, we estimate the average infiltration rate as 0.2 air
 409 changes per hour (ACH) in summer based on some previous research (Chen and Zhao 2011; G.
 410 Hong and Kim 2016). According to the volume of the room and the outdoor pollutant concentration,
 411 the air infiltration process might cause the indoor ozone level to raise to 8 ppb during the night. As

412 can be seen in Figure 5, the measured indoor ozone concentration stayed around 10 ppm during
413 the night when the windows were closed, which was supposed to be associated with the air
414 infiltration. Therefore, the actual indoor pollutant concentration considering the air infiltration
415 would be 5% higher than the simulated results in this work, which results in a higher IAQ index
416 and thus higher exposure risk than evaluated.

417 As for the concept of the exposure injury, in the current work, we focus more on the indoor air
418 quality and the corresponding respiratory dosage and deposition through breathing. As concluded
419 in Table 2, a qualitative evaluation indicates the significant potential of wheezing and shortness of
420 breath in people with asthma, as well as the increasing of lung disease, under the calculated IAQ
421 index. However, quantitative analysis of the contaminant penetrating into the blood through layers
422 of skin, stratum corneum, viable epidermis and dermal capillaries is also necessary to carry out
423 together with the physiological researches in the next step, to determine the exact injury level.
424 Recently, a model of transdermal uptake of hazardous chemicals has been raised by Morrison et
425 al. in 2017. The final mass of the gaseous chemicals (e.g., SO₂, CO) entered the blood can be
426 calculated based on the dynamic indoor chemical concentration as a boundary condition. But the
427 key point is to validate the aforementioned model with a set of proper parameters for specific
428 gaseous contaminants.

429 As for the selection of airborne particle metrics, ultrafine particles also play a non-negligible
430 role in affecting the occupant health, especially to the respiratory system due to its smaller particle
431 size (Ibald-Mulli et al. 2002; Zhao et al. 2009; Nikolova et al. 2011). Plus that the physical
432 diffusion process (origin, dynamic and penetration) between PM_{2.5} and ultrafine particles are
433 actually different. Therefore, the approach proposed in this work is a simplified approach for not
434 considering the ultrafine particles in the overall framework. To address this problem, accurate

435 measured ultrafine particles data should be collected via carefully designed experiments, to further
436 validate the physical models of their diffusion process.

437 The methodology in this paper is more targeting at the commercial building types (namely,
438 office buildings) where many indoor pollutant sources such as cooking and incense could be
439 negligible. When it comes to residential building types for a broader application, the simulation of
440 indoor combustion sources should be added to the current methodology, especially the CFD
441 simulation of the origin, dynamics and penetration of such particle metrics (Yang and Ye 2014;
442 Ezzati and Kammen 2001).

443

444 **Conclusion**

445 This work employed both whole-building simulation (EnergyPlus coupled with obFMU) and
446 computational fluid dynamics (Fluent) to analyze the impacts of occupant behaviors (namely
447 window operation, HVAC operation, and human movements) on indoor airflow patterns and IAQ.
448 The IAQ, especially considering daily occupant behavior schedules, was assessed during the
449 period of a wildfire event in the Northern California, U.S.

450 The simulated results were compared with the actual measured indoor and outdoor data (O₃ and
451 PM_{2.5}). The measured and simulated IAQ were consistent based on the maximum and average
452 levels. The occupant behaviors were proved to exert significant impacts on the indoor air flow
453 pattern and thus the pollutants' concentrations. The indoor airflow pattern and IAQ transformed
454 obviously within working hours, which were largely dependent on occupant behaviors. Thus, to
455 mitigate indoor exposure risk, occupants are advised to keep windows closed and operate HVAC
456 systems without outdoor air. Besides, occupants' movements accelerate the diffusion and mixture
457 of existing contaminants at different heights, which could enhance the risk of respiratory exposure.

458 The daily maximum IAQ index was 215, with SO₂ as the responsible pollutant, which might result
459 in significant respiratory symptoms and adverse health effects, such as wheezing and shortness of
460 breath, in children, older adults, and people with asthma. Based on indoor air conditions and
461 considering occupant behaviors, deposit fraction and equation were fitted to predict the respiratory
462 injury level under such outdoor wildfire conditions.

463 This study formulated a framework for the indoor pollutants exposure modeling and the potential
464 human health hazard assessment in an office environment while taking into account actual
465 occupant behaviors. This co-simulation was conducted by combining the building energy
466 modeling, occupant behavior modeling, CFD modeling, and pollutant modeling, which can be
467 further applied in each IAQ issue where the outdoor-to-indoor pollutant penetration aspect is
468 important (such as wildfire events as demonstrated in this work, haze pollution in China, as well
469 as the vehicle exhaust etc). Results can be used to evaluate and inform strategies to mitigate
470 occupant health conditions during outdoor events of extreme pollution.

471

472 **References:**

- 473 Anderson CM, Kissel KA, Field CB, Mach KJ (2018). Climate Change Mitigation, Air
474 Pollution, and Environmental Justice in California. *Environmental Science & Technology*,
475 52(18): 10829–38.
- 476 Chen C, Zhao B (2011). Review of Relationship between Indoor and Outdoor Particles: I/O
477 Ratio, Infiltration Factor and Penetration Factor. *Atmospheric Environment*,
478 <https://doi.org/10.1016/j.atmosenv.2010.09.048>.
- 479 Chen Y, Hong T, Luo X (2018). An Agent-Based Stochastic Occupancy Simulator. *Building*
480 *Simulation*,. <https://doi.org/10.1007/s12273-017-0379-7>.

481 Crawley DB, Lawrie LK, Winkelmann FC, Buhl WF, Huang YJ, Pedersen CO, Strand RK,
482 Liesen RJ, Fisher DE, Witte MJ, Glazer J (2001). EnergyPlus: Creating a New-Generation
483 Building Energy Simulation Program. *Energy and Buildings*,.
484 [https://doi.org/10.1016/S0378-7788\(00\)00114-6](https://doi.org/10.1016/S0378-7788(00)00114-6).

485 Ezzati M, Kammen DM (2001). Quantifying the Effects of Exposure to Indoor Air Pollution
486 from Biomass Combustion on Acute Respiratory Infections in Developing Countries.
487 *Environmental Health Perspectives*, 109(5): 481–88.

488 Fracastoro GV, Mutani G, Perino M (2002). Experimental and Theoretical Analysis of Natural
489 Ventilation by Windows Opening. In *Energy and Buildings*,. [https://doi.org/10.1016/S0378-](https://doi.org/10.1016/S0378-7788(02)00099-3)
490 [7788\(02\)00099-3](https://doi.org/10.1016/S0378-7788(02)00099-3).

491 Gosselin JR, Chen Q (Yan) (2008). A Computational Method for Calculating Heat Transfer and
492 Airflow through a Dual-Airflow Window. *Energy and Buildings*,.
493 <https://doi.org/10.1016/j.enbuild.2007.03.010>.

494 Haddrell AE, Davies JF, Reid JP (2015). Dynamics of Particle Size on Inhalation of
495 Environmental Aerosol and Impact on Deposition Fraction. *Environmental Science and*
496 *Technology*,. <https://doi.org/10.1021/acs.est.5b01930>.

497 Haikerwal A, Akram M, Monaco A Del, Smith K, Sim MR, Meyer M, Tonkin AM, Abramson
498 MJ, Dennekamp M (2015). Impact of Fine Particulate Matter (PM2.5) Exposure during
499 Wildfires on Cardiovascular Health Outcomes. *Journal of the American Heart Association*,.
500 <https://doi.org/10.1161/JAHA.114.001653>.

501 Haldi F (2013). A Probabilistic Model To Predict Building Occupants' Diversity Towards Their
502 Interactions With the Building Envelope. *Proceedings of the International IBPSA*
503 *Conference*,.

504 Han Z, Weng W, Huang Q (2014). Numerical and Experimental Investigation on the Dynamic
505 Airflow of Human Movement in a Full-Scale Cabin. In *HVAC and R Research*,
506 <https://doi.org/10.1080/10789669.2014.882677>.

507 Hong G, Kim BS (2016). Field Measurements of Infiltration Rate in High Rise Residential
508 Buildings Using the Constant Concentration Method. *Building and Environment*,
509 <https://doi.org/10.1016/j.buildenv.2015.11.027>.

510 Hong T, D'Oca S, Taylor-Lange SC, Turner WJN, Chen Y, Corgnati SP (2015). An Ontology to
511 Represent Energy-Related Occupant Behavior in Buildings. Part II: Implementation of the
512 DNAS Framework Using an XML Schema. *Building and Environment*,
513 <https://doi.org/10.1016/j.buildenv.2015.08.006>.

514 Hong T, D'Oca S, Turner WJN, Taylor-Lange SC (2015). An Ontology to Represent Energy-
515 Related Occupant Behavior in Buildings. Part I: Introduction to the DNAs Framework.
516 *Building and Environment*, <https://doi.org/10.1016/j.buildenv.2015.02.019>.

517 Hong T, Sun H, Chen Y, Taylor-Lange SC, Yan D (2016). An Occupant Behavior Modeling
518 Tool for Co-Simulation. *Energy and Buildings*,
519 <https://doi.org/10.1016/j.enbuild.2015.10.033>.

520 Hong T, Yan D, D'Oca S, Chen C fei (2017). Ten Questions Concerning Occupant Behavior in
521 Buildings: The Big Picture. *Building and Environment*,
522 <https://doi.org/10.1016/j.buildenv.2016.12.006>.

523 Hurteau MD, Westerling AL, Wiedinmyer C, Bryant BP (2014). Projected Effects of Climate
524 and Development on California Wildfire Emissions through 2100. *Environmental Science*
525 *& Technology*, 48(4): 2298–2304.

526 Ibald-Mulli A, Wichmann H-E, Kreyling W, Peters A (2002). Epidemiological Evidence on

527 Health Effects of Ultrafine Particles. *Journal of Aerosol Medicine*, 15(2): 189–201.

528 Jaffe DA, Wigder N, Downey N, Pfister G, Boynard A, Reid SB (2013). Impact of Wildfires on
529 Ozone Exceptional Events in the Western US. *Environmental Science & Technology*,
530 47(19): 11065–72.

531 Jolly WM, Cochrane MA, Freeborn PH, Holden ZA, Brown TJ, Williamson GJ, Bowman DMJS
532 (2015). Climate-Induced Variations in Global Wildfire Danger from 1979 to 2013. *Nature*
533 *Communications*, 6: 7537.

534 Klepeis NE, Nelson WC, Ott WR, Robinson JP, Tsang AM, Switzer P, Behar J V, Hern SC,
535 Engelmann WH (2001). The National Human Activity Pattern Survey (NHAPS): A
536 Resource for Assessing Exposure to Environmental Pollutants. *Journal of Exposure Science*
537 *and Environmental Epidemiology*, 11(3): 231.

538 Lewis TC, Robins TG, Mentz GB, Zhang X, Mukherjee B, Lin X, Keeler GJ, Dvonch JT, Yip
539 FY, O’Neill MS (2013). Air Pollution and Respiratory Symptoms among Children with
540 Asthma: Vulnerability by Corticosteroid Use and Residence Area. *Science of the Total*
541 *Environment*, 448: 48–55.

542 Lin B, Huangfu Y, Lima N, Jobson B, Kirk M, O’Keeffe P, Pressley S, Walden V, Lamb B,
543 Cook D (2017). Analyzing the Relationship between Human Behavior and Indoor Air
544 Quality. *Journal of Sensor and Actuator Networks*,. <https://doi.org/10.3390/jsan6030013>.

545 Luo N, Weng W, Xu X, Fu M (2018a). Experimental and Numerical Investigation of the Wake
546 Flow of a Human-Shaped Manikin: Experiments by PIV and Simulations by CFD. *Building*
547 *Simulation*,. <https://doi.org/10.1007/s12273-018-0446-8>.

548 ——— (2018b). Human-Walking-Induced Wake Flow – PIV Experiments and CFD
549 Simulations. *Indoor and Built Environment*,. <https://doi.org/10.1177/1420326X17701279>.

550 Luongo JC, Fennelly KP, Keen JA, Zhai ZJ, Jones BW, Miller SL (2016). Role of Mechanical
551 Ventilation in the Airborne Transmission of Infectious Agents in Buildings. *Indoor Air*,
552 <https://doi.org/10.1111/ina.12267>.

553 Mintz D (2013). Technical Assistance Document for the Reporting of Daily Air Quality – the Air
554 Quality Index (AQI). *Environmental Protection*,.

555 Montgomery JF, Storey S, Bartlett K (2015). Comparison of the Indoor Air Quality in an Office
556 Operating with Natural or Mechanical Ventilation Using Short-Term Intensive Pollutant
557 Monitoring. *Indoor and Built Environment*,. <https://doi.org/10.1177/1420326X14530999>.

558 Morrison GC, Weschler CJ, Bekö G (2017). Dermal Uptake of Phthalates from Clothing:
559 Comparison of Model to Human Participant Results. *Indoor Air*,
560 <https://doi.org/10.1111/ina.12354>.

561 Navarro KM, Cisneros R, O’Neill SM, Schweizer D, Larkin NK, Balmes JR (2016). Air-Quality
562 Impacts and Intake Fraction of PM_{2.5} during the 2013 Rim Megafire. *Environmental
563 Science & Technology*, 50(21): 11965–73.

564 Newsham GR (1994). Manual Control of Window Blinds and Electric Lighting: Implications for
565 Comfort and Energy Consumption. *Indoor and Built Environment*,
566 <https://doi.org/10.1177/1420326X9400300307>.

567 Nikolova I, Janssen S, Vos P, Vrancken K, Mishra V, Berghmans P (2011). Dispersion
568 Modelling of Traffic Induced Ultrafine Particles in a Street Canyon in Antwerp, Belgium
569 and Comparison with Observations. *Science of the Total Environment*, 412: 336–43.

570 Shi S, Chen C, Zhao B (2015). Air Infiltration Rate Distributions of Residences in Beijing.
571 *Building and Environment*,. <https://doi.org/10.1016/j.buildenv.2015.05.027>.

572 Stabile L, Dell’Isola M, Russi A, Massimo A, Buonanno G (2017). The Effect of Natural

573 Ventilation Strategy on Indoor Air Quality in Schools. *Science of the Total Environment*,
574 <https://doi.org/10.1016/j.scitotenv.2017.03.048>.

575 West JJ, Smith SJ, Silva RA, Naik V, Zhang Y, Adelman Z, Fry MM, Anenberg S, Horowitz
576 LW, Lamarque J-F (2013). Co-Benefits of Mitigating Global Greenhouse Gas Emissions
577 for Future Air Quality and Human Health. *Nature Climate Change*, 3(10): 885.

578 WHO (2010). WHO Guidelines for Indoor Air Quality: Selected Pollutants. *Bonn, Germany: In*
579 *Puncto Druck+ Medien GmbH*,. <https://doi.org/10.1186/2041-1480-2-S2-I1>.

580 World Health Organization (2005). WHO Air Quality Guidelines for Particulate Matter, Ozone,
581 Nitrogen Dioxide and Sulfur Dioxide: Global Update 2005. *World Health Organization*,.
582 [https://doi.org/10.1016/0004-6981\(88\)90109-6](https://doi.org/10.1016/0004-6981(88)90109-6).

583 Xu X, Shang Y, Tian L, Weng W, Tu J (2018). A Numerical Study on Firefighter Nasal Airway
584 Dosimetry of Smoke Particles from a Realistic Composite Deck Fire. *Journal of Aerosol*
585 *Science*, 123: 91–104.

586 Yang L, Ye M (2014). CFD Simulation Research on Residential Indoor Air Quality. *Science of*
587 *the Total Environment*, 472: 1137–44.

588 You S, Yao Z, Dai Y, Wang CH (2017). A Comparison of PM Exposure Related to Emission
589 Hotspots in a Hot and Humid Urban Environment: Concentrations, Compositions,
590 Respiratory Deposition, and Potential Health Risks. *Science of the Total Environment*,.
591 <https://doi.org/10.1016/j.scitotenv.2017.04.217>.

592 Zhang Z, Chen X, Mazumdar S, Zhang T, Chen Q (2009). Experimental and Numerical
593 Investigation of Airflow and Contaminant Transport in an Airliner Cabin Mockup. *Building*
594 *and Environment*,. <https://doi.org/10.1016/j.buildenv.2008.01.012>.

595 Zhao B, Chen C, Tan Z (2009). Modeling of Ultrafine Particle Dispersion in Indoor

596 Environments with an Improved Drift Flux Model. *Journal of Aerosol Science*, 40(1): 29–
597 43.

598

599 **Acknowledgements:**

600 We thank the Indoor Environment Group of Lawrence Berkeley National Laboratory for providing the
601 measured indoor and outdoor air quality data. This study was supported by National Key R&D Program of
602 China (Grant No. 2016YFC0802801 and 2016YFC0802807), National Science Fund for Distinguished
603 Young Scholars of China (Grant No 71725006), National Natural Science Foundation of China (Grant No.
604 51706123). This work was also supported by the Office of Energy Efficiency and Renewable Energy, the
605 United States Department of Energy under Contract No. DE-AC02-05CH11231. The authors are deeply
606 grateful to these supports.

607

608

609 **Author contributions:**

610 N.L., W.W. and T.H. designed the study. N.L., X.X. and K.S. conducted the combined simulation of the
611 OB-based indoor environment. All authors participated in writing and revising the manuscript. All authors
612 read and approved the submitted manuscript.